

Slow dynamics in gelation phenomena: From chemical gels to colloidal glasses

Emmanuel Del Gado,^{a,d}, Annalisa Fierro,^{b,d}, Lucilla de Arcangelis,^{c,d} and Antonio Coniglio^{b,d}^aLaboratoire des Verres, Université Montpellier II, 34095 Montpellier, France^bDipartimento di Scienze Fisiche, Università di Napoli "Federico II",

Complesso Universitario di Monte Sant'Angelo, via Cintia 80126 Napoli, Italy

^cDipartimento di Ingegneria dell'Informazione, Seconda Università di Napoli,

via Roma 29, 81031 Aversa (Caserta), Italy and

^dINFN Udr di Napoli and Gruppo coordinato SUN

(Dated: April 14, 2024)

We here discuss the results of 3d Monte Carlo simulations of a minimal lattice model for gelling systems. We focus on the dynamics investigated by means of the time autocorrelation function of the density fluctuations and the particle mean square displacement. We start from the case of chemical gelation, i.e. with permanent bonds, and characterize the critical dynamics as determined by the formation of the percolating cluster, as actually observed in polymer gels. By opportunely introducing a finite bond lifetime τ_b , the dynamics displays relevant changes and eventually the onset of a glassy regime. This has been interpreted in terms of a crossover to dynamics more typical of colloidal systems and a novel connection between classical gelation and recent results on colloidal systems is suggested. By systematically comparing the results in the case of permanent bonds to finite bond lifetime, the crossover and the glassy regime can be understood in terms of effective clusters.

I. INTRODUCTION

The gelation transition transforms a viscous liquid into an elastic disordered solid. In general this is due to the formation in the liquid phase of a spanning structure, which makes the system able to bear stresses. In polymer systems, this is due to chemical bonding, that can be induced in different ways [1, 2], producing a polymerization process. As firstly recognized by Flory, the change in the viscoelastic properties is directly related to the constitution inside the sol of a macroscopic polymeric structure, that characterizes the gel phase. In experiments [3] the viscosity coefficient grows as a power law as function of the relative difference from the critical polymer concentration with a critical exponent k . The onset of the elastic response in the system, as function of the same control parameter, displays a power law increasing of the elastic modulus with a critical exponent f . As implicitly suggested in the work of Flory and Stockmayer [1], the percolation model is considered as the basic model for the chemical gelation transition and the macro-molecular stress-bearing structure in these systems is a percolating network [2, 4, 5]. In experiments the gelling solution typically displays slow dynamics: the relaxation functions present a long time stretched exponential decay $e^{-(\frac{t}{\tau})^\alpha}$ as the gelation threshold is approached. In particular at the gel point the relaxation process becomes critically slow, and the onset of a power law decay is observed [6].

In many other physical systems where aggregation processes and structure formation take place, gelation phenomena can be observed. Typically, these are colloidal systems, i.e. suspensions of mesoscopic particles interacting via short range attraction. These systems are intensively investigated due to their relevance in many research fields (from proteins studies to food industry).

Due to the possibility in experiments of opportunely tuning the features of the interactions, they also play the role of model systems.

In these systems strong attraction gives rise to a diffusion limited cluster-cluster aggregation process and may produce gel formation (colloidal gelation) at very low density as a spanning structure is formed [7]. The latter is generally quite different from the polymer gels case [8] however, for what the viscoelastic behavior is concerned, this gelation transition closely resembles the chemical one, observed in polymer systems [9]. With a weaker attraction at higher densities a gelation characterized by a glass-like kinetic arrest [10, 11] may be observed. The relaxation patterns closely recall the ones observed in glassy systems and are well fitted by the mode-coupling theory predictions for super-cooled liquids approaching the glass transition [12]. On the theoretical side the application of the mode-coupling theory to systems with short range attractive interactions [13, 14, 15] (attractive glasses) has been recently considered and the connection with the colloidal glass transition has been proposed. The short range attraction enhances the caging mechanism characteristic of glassy regimes in hard sphere systems and produces a glassy behavior at lower densities, depending on the attraction strength.

At lower densities, the role of the structure formation, as directly observed in some systems [16], might be relevant in the dynamics but it has not been clarified yet. Also the eventual crossover to the glassy regime [9], as the density is increased, is not completely understood. In this paper we investigate the connection among colloidal gelation, colloidal glass transition and chemical gelation. Some preliminary studies have been reported in [17].

We have considered a minimal model for gelling systems and performed extensive numerical simulations on 3d cubic lattices. In Sect. II we give the details of the model and the simulations. In Sect.s III and IV the re-

sults relative to relaxation and diffusion properties are presented and discussed. In the last section some concluding remarks are given.

II. DESCRIPTION OF THE MODEL

A. Permanent bonds

Our model consists in a solution of monomers diffusing on a cubic lattice. As in most experimental polymer gels, we choose the monomers to be tetrafunctional. Each monomer occupies a lattice elementary cell, and therefore eight vertices on the lattice. To take into account the excluded volume interaction, two monomers cannot occupy nearest neighbors and next nearest neighbors cells on the lattice, i.e. nearest neighbor monomers cannot have common sites. At $t = 0$ we fix the fraction ϕ of present monomers with respect to the maximum number allowed on the lattice, and randomly quench bonds between them. This actually corresponds to the typical chemical gelation process that can be obtained by irradiating the monomeric solution. We form at most four bonds per monomer, randomly selected along lattice directions and between monomers that are nearest neighbors and next nearest neighbors (namely bond lengths $l = 2; 3$). Once formed, the bonds are permanent.

For each value of ϕ there is an average value $N_b(\phi)$ of the fraction of formed bonds with respect to all the possible ones, obtained by averaging over different initial configurations.

Varying ϕ the system presents a percolation transition at $\phi_c = 0.718 \pm 0.005$ [18]. The critical exponents found at the transition agree with the random percolation predictions [19] (e.g. for the mean cluster size $\gamma' = 1.8 \pm 0.05$ and for the correlation length $\nu' = 0.89 \pm 0.01$ in 3d [18]).

The monomers diffuse on the lattice via random local movements and the bond length may vary but not be larger than l_0 according to bond fluctuation dynamics (BFD) [20], where the value of l_0 is determined by the self-avoiding walk condition. On the cubic lattice we have $l_0 = \sqrt{10}$ in lattice spacing units and the allowed bond lengths are $l = 2; 5; 6; 3; 10$ [21]. We let the monomers diffuse to reach the stationary state and then study the system for different values of the monomer concentration.

This lattice model with permanent bonds has been introduced to study the critical behavior of the viscoelastic properties at the gelation transition [22]. The relaxation time is found to diverge at the percolation threshold ϕ_c with a power law behavior [18]. The elastic response in the gel phase has been studied by means of the fluctuations in the free energy and goes to zero at ϕ_c with a power law behavior as well [23].

B. Bonds with finite lifetime

Colloidal gelation is due to a short range attraction and in general the particles are not permanently bonded. To take into account this crucial feature we introduce a novel ingredient in the previous model by considering a finite bond lifetime τ_b and study the effect on the dynamics.

The features of this model with finite τ_b can be realized in a microscopic model: a solution of monomers interacting via an attraction of strength E and excluded volume repulsion. Due to monomer diffusion the aggregation process eventually takes place. The finite bond lifetime τ_b is related to the attractive interaction of strength E , as $\tau_b = e^{E/kT}$.

We start with the same configurations of the previous case, with a fixed ϕ where the bonds have been randomly quenched as described above. During the monomer diffusion with BFD at every time step we attempt to break each bond with a frequency $1 = \tau_b$. Between monomers separated by a distance less than l_0 bonds are then formed with a frequency f_b [24]. In order to obtain monomer configurations that are similar to the ones with permanent bonds, for each value of ϕ we fix f_b so that the fraction of present bonds coincides with its average value in the case of permanent bonds, $N_b(\phi)$ [26].

With respect to the case of permanent bonds we notice that, as the finite bond lifetime τ_b corresponds to an attractive interaction of range l_0 , it actually introduces a correlation in the bond formation and may eventually lead to a phase separation between a low density and a high density phase: There is no evidence of phase separation for the values of τ_b and f_b considered in this paper. This is evident in Fig.1, where typical equilibrium configurations with $\phi = 0.6$ are shown in two different cases: in Fig.1(a) we have the case considered in this paper, obtained with $\tau_b = 100$ and $f_b = 0.02$; in Fig.1(b) with $\tau_b = 2$ and $f_b = 1$ the phase separation may occur. The choice of monomers of functionality 4, also in this case of finite bond lifetime, may correspond to a directional effect in the interaction [27].

The case of extremely large τ_b gives rise to different situations depending on the initial condition and the bond creation process. We consider two extreme cases: I) Start with the initial configuration where the monomers are randomly distributed, and the bonds are randomly quenched. At later times the frequency of forming bonds is zero. This case corresponds to the permanent bond case (chemical gelation), described in section IIA. II) Start with a random configuration of monomers and let the monomers diffuse and form bonds with finite lifetime and frequency f_b . This phenomenon of irreversible aggregation, with the occurrence of gelation after a spanning cluster is formed, corresponds to cluster-cluster aggregation class of models for $f_b = 1$ [28], with a tendency towards cluster-cluster reaction limited aggregation process [29] for $f_b < 1$. This out of equilibrium phenomenon can be representative of colloidal gelation and will not be considered here. In chemical gelation and colloidal

gelation the formation of the critical cluster should produce the slow dynamics. The main difference is due to the fact that the critical density and the temperature are much lower in colloidal gelation than in chemical gelation, moreover the fractal dimension is related to cluster-cluster aggregation models and not to random percolation.

III. RELAXATION FUNCTIONS

In order to investigate the dynamic behavior we study, for both the permanent bond and the finite bond lifetime cases, the equilibrium density fluctuation autocorrelation functions, $f_q(t)$, given by

$$f_q(t) = \frac{\langle \varphi_q(t + t^0) \varphi_q(t^0) \rangle}{\langle |\varphi_q(t^0)|^2 \rangle} \quad (1)$$

where $\varphi_q(t) = \frac{1}{N} \sum_{i=1}^N e^{iq \cdot \mathbf{r}_i(t)}$, $\mathbf{r}_i(t)$ is the position of the i th monomer at time t , N is the number of monomers and the average $\langle \dots \rangle$ is performed over the time t^0 . Due to periodic boundary conditions the values of the wave vector q on the cubic lattice are $q = \frac{2\pi}{L} (n_x; n_y; n_z)$ with $n_x, n_y, n_z = 1; \dots; L/2$ integer values (in our simulations a cubic lattice of size $L = 16$ has been considered) [30]. In the following we discuss the data obtained for $q = (1; 3; 6)$ ($q = (-4; -4; -4)$). Qualitatively analogous behaviors have been observed for $q = (-2; -2; -2)$ and $(1; 1; 1)$. Undoubtedly, due to structure formation over different length scales, a detailed study of the geometric properties and the dynamics for different wave vectors might be relevant [31].

In the case of permanent bonds the system is considered at equilibrium when both the diffusion coefficient has reached its asymptotic limit, and the autocorrelation functions have gone to zero. For $\phi < \phi_c$ we are always able to thermalize the system, instead for $\phi > \phi_c$ it remains out of equilibrium, and it is possible that it is in an aging regime [31]. In Fig 2, $f_q(t)$ is plotted as function of the time for different values of the monomer concentration. The data have been averaged over 40 different initial configurations. The different curves correspond to different values of ϕ , ranging from 0.5 to 0.85. At low concentrations the system completely relaxes within the simulation time; the relaxation process becomes slower as the concentration is increased and above the percolation threshold, ϕ_c , the system is kinetically arrested, in the sense that the relaxation functions do not go to zero within the time scale of the simulations.

We analyze more quantitatively the long time decay of $f_q(t)$ in Fig.3: As the monomer concentration, ϕ , approaches the percolation threshold, ϕ_c , $f_q(t)$ displays a long time decay well fitted by a stretched exponential law $e^{-(t/\tau)^\alpha}$ with $\alpha = 0.30 \pm 0.05$. Intuitively, this behavior can be related to the cluster size distribution close to the gelation threshold, which produces relaxation processes taking place over different length scales. At

the percolation threshold the onset of a power law decay (with an exponent c) is observed as shown by the double logarithmic plot of Fig.3 [6]. As the monomer concentration is increased above the percolation threshold, i.e. in the gel phase, the long time power law decay of the relaxation functions can be fitted with a decreasing exponent c , varying from $c = 1.0$ at ϕ_c to $c = 0.2$ well above ϕ_c , where a nearly logarithmic decay appears. This suggests that the growth of the relaxation time is driven by the formation of the critical cluster, that actually determines the kinetic arrest. On the whole, this behavior well agrees with the one observed in gelling systems investigated in the experiments of refs.[6]. It is interesting to notice that this kind of decay with a stretched exponential and a power law reminds the relaxation behavior found in spin-glasses [32]. Many analogies in the dynamics of gels and spin-glasses have been recently pointed out [33], but the underlying physics is rather unclear.

In the model with finite lifetime bonds, the equilibration time is an increasing function of ϕ_b . The system is considered at equilibrium when both the average number of bonds has reached its asymptotic limit and the autocorrelation functions have gone to zero [34]. In this case very different behaviors are observed. In Fig.4 $f_q(t)$ is plotted as function of time for a fixed value of $\phi_b = 10; 100; 1000$ (respectively Fig.4a, 4b and 4c) for increasing values of the monomer concentration (ϕ varies on the same range as the permanent bond case). At low concentrations, the behavior of the autocorrelation function $f_q(t)$ is apparently very similar to the one observed in the case of permanent bonds: the system completely relaxes within the simulation time scale and the relaxation time increases with the concentration. At high concentrations, a two-step decay appears, closely resembling the one observed in super-cooled liquids. This qualitative behavior is observed for many different values of the bond lifetime, ϕ_b . As shown in Fig. 4, the two step decay is more pronounced for higher values of ϕ_b .

As we can see in Fig.5, where the long time decay of $f_q(t)$ for $\phi_b = 100$ is shown, the long time decays are well fitted by stretched exponentials. The exponent ($\alpha = 0.7$ for the case of Fig.5) does not seem to vary significantly as the concentration varies, and this has been observed for all the values of ϕ_b studied. It instead decreases as ϕ_b increases: for very small ϕ_b one recovers a long time exponential decay whose behavior becomes less and less exponential as the bond lifetime increases. This suggests that the stretched exponential decay is due to the presence of long living structures.

For high monomer concentrations we fit the $f_q(t)$ curves using the mode-coupling correlator [12], corresponding to a short time power law $f + \frac{t}{\tau_1}^a$ and a long time von Schweidler law $f - \frac{t}{\tau_2}^b$. In Fig.6 we show the agreement between the fit (the full lines) and the data for $\phi_b = 1000$ in the range of concentrations $\phi = 0.8 \pm 0.9$. The exponents obtained are $a = 0.33 \pm 0.01$

and $b = 0.65 \pm 0.01$. At long times the different curves obtained for different ϕ collapse onto a unique master curve by opportunistically rescaling the time via a factor ϕ^{-1} (Fig.7). The master curve is well fitted by a stretched exponential decay with $\beta = 0.50 \pm 0.06$. The characteristic time $\tau_g(\phi)$ diverges at a value $\phi_g = 0.963 \pm 0.005$ with the exponent 2.33 ± 0.06 (Fig.8). This value well agrees with the mode-coupling prediction $\phi_g = 1/2a + 1/2b$ [12].

The same behavior and the same level of agreement between the data and the mode coupling predictions have been obtained for different values of b ($b = 100; 200; 400; 1000; 3000$). Neither the exponents a and b obtained by the α -correlator nor the exponent β of the stretched exponential vary significantly as function of ϕ and of b . The value of τ_g , where the characteristic time $\tau_g(\phi)$ apparently diverges, seems instead to vary with b , but it is always close to $\tau_g = 1$.

This glassy relaxation pattern suggests that also in this case the relaxation takes place by means of a caging mechanism: particles are trapped in a cage formed by the surrounding ones, the first relaxation step is due to movements within this cage, whereas the final relaxation is possible due to cage opening and rearrangement. We notice that, contrary to the usual behavior observed in super-cooled liquids and predicted by the Mode-Coupling Theory, the value of the plateau of the relaxation functions, which is typically related to the size of the cage, strongly depends on the monomer concentration, ϕ . This effect will be explained later in terms of effective clusters.

IV. THE RELAXATION TIME AND THE ROLE OF EFFECTIVE CLUSTERS

We study now the relaxation times that can be obtained from the $f_q(t)$, as the time τ_q such that $f_q(\tau_q) = 0.1$. In Fig.9 the relaxation time τ_q is plotted as function of the monomer concentration, ϕ , for the permanent bonds and for the finite lifetime bonds case at different values of b . In the figure one finds the data for the permanent bond case on the left, and then from left to right the data for decreasing values of bond lifetime, b .

In the case of permanent bonds (chemical gelation), $\tau_q(\phi)$ displays a power law divergence at the percolation threshold ϕ_c . For finite bond lifetime the relaxation time instead increases following the permanent bond case, up to some value ϕ_g and then deviates from it. The longer the bond lifetime the higher ϕ_g is. For higher ϕ_g the further increase of the relaxation time corresponds to the onset of the glassy regime in the relaxation behavior discussed in the previous section. This truncated critical behavior followed by a glassy-like transition has been actually detected in some colloidal systems in the viscosity behavior [35, 36].

In both cases of permanent bonds and finite lifetime bonds, clusters of different sizes are present in the system. In the permanent bond case, a cluster of radius R diffuses in the medium formed by the other percola-

tion clusters with a characteristic relaxation time $\tau(R)$. At the percolation threshold the connectedness length critically grows in the system and so does the overall relaxation time. In the case of a finite bond lifetime b , it will exist a cluster size R so that $b < \tau(R)$. That is, clusters of size $R \approx R_c$ will break and lose their identity on a time scale shorter than $\tau(R)$ and their full size will not contribute to the enhancement of the relaxation time in the system. We can say that the finite bond lifetime actually introduces an effective cluster size distribution with a cut-off and keeps the macroscopic viscosity finite in the system [37].

At high concentrations the system approaches a glassy regime and the relaxation time increases. In order to further investigate the high concentration regime, in Fig.10 we directly compare $f_q(t)$ at fixed $\phi = 0.85$ for $b = 10; 100; 400; 1000$, and the permanent bond case. We observe that at a fixed value of the monomer concentration, ϕ , the relaxation functions calculated for finite lifetime bonds coincide with the permanent bond case up to times of the order of b . This suggests that on time scales smaller than b the relaxation process must be on the whole the same as in the case of permanent bonds, where permanent clusters are present in the system, and gives an interpretation in terms of effective clusters for the two step glassy behavior of the relaxation functions: The first step is due to the relaxation of a cluster within the cage formed by the other clusters, whereas the second step is due to the breaking of clusters. This second relaxation is the analog of the cage opening in an ordinary supercooled liquid. In conclusion, on a time scale of the order of b , the effective clusters play the role of single molecules in an ordinary supercooled liquid, or in a colloidal hard sphere system.

Using this picture of effective clusters, we are able to explain the increase of the plateau in $f_q(t)$. In fact, since different values of the monomer concentration correspond to different effective cluster size distributions, for each value of ϕ one has a different glassy liquid of effective clusters. This will change the first relaxation and should correspond to a change in the plateau of the relaxation functions (Fig.4 and 6). In particular we find that for higher ϕ one has a higher plateau, that is the first decay (the motion of clusters within the cages) produces a smaller relaxation in the system.

V. DIFFUSION PROPERTIES

In order to obtain further information on the dynamics we calculate the mean square displacement of all the particles, $\overline{h^2(t)} = \frac{1}{N} \sum_{i=1}^N \overline{(r_i(t) - r_i(t^0))^2}$. In the model with finite lifetime bonds, clusters continuously evolve in time and therefore the diffusion coefficient of a single cluster cannot be defined.

In the model with permanent bonds the mean square displacement of the particles $\overline{h^2(t)}$ presents a long-time diffusive behavior, and the diffusion coefficient decreases

but remains finite also above ϕ_c . This is due to the fact that the infinite cluster can be viewed as a net with a large mesh size, through which monomers and small clusters can diffuse.

In previous papers [18] the diffusion coefficient of clusters with a fixed size was studied. We found that clusters, whose size is comparable with the connectedness length, present a diffusion coefficient going to zero at ϕ_c (with the same exponent as the relaxation time), whereas single monomers present a finite diffusion coefficient also in the gel phase. As we have already noticed, this is due to the fact that small clusters are able to escape through the percolating cluster having a structure with holes over many different length scales close to the percolation threshold. It is therefore clear that the behavior here observed for the mean square displacement is mainly due to the diffusion of single monomers and small clusters. In Fig.11, $\langle r^2(t) \rangle$ is plotted as function of time in a double logarithmic plot for ϕ approaching ϕ_c in the case of permanent bonds: particles can still diffuse, and the diffusion coefficient apparently decreases with the monomer concentration. At high concentrations the sub-diffusive regime stays longer, and the long time diffusive behavior is hardly recovered.

In Fig.12, we plot the data obtained with $b = 1000$ and $\phi = 0.8; 0.82; 0.85; 0.9$. According to the results just discussed, for low concentrations $\langle r^2(t) \rangle$ shows a simple diffusive behavior. The diffusion does not change significantly close to ϕ_c and for high concentrations the behavior observed, characterized by a plateau, is similarly to glass forming systems. This onset of a glassy regime has been obtained for different values of b , and again it indicates a caging mechanism in the dynamics. The asymptotic diffusion coefficient goes to zero as ϕ approaches ϕ_g (inset of Fig.12), as a power law, with an exponent close to -1 (section IV) in agreement with the Mode Coupling Theory predictions.

As already done for the relaxation functions we directly compare the mean square displacement obtained in the cases of permanent bonds and finite bond lifetime. Fig.13 shows for a fixed value of the concentration, $\phi = 0.85$, that the two quantities coincide up to time scales of the order of b . For longer times in the system with non permanent bonds the normal diffusive regime is recovered. These results are coherent with the behavior of the relaxation functions discussed in the previous section. The

first regime is apparently related to the diffusion of effective clusters. Here again the value of the plateau in the diffusion pattern, which is related to the size of the cage, varies with the concentration. For higher values of the monomer concentration, the size of the cage apparently decreases. This corresponds to larger effective clusters, which have less free space compared to their size. By means of the qualitative argument used in section IV,

one expects that for a longer b the condition $b < (R_c)$ will be fulfilled by a larger size R_c , and on average larger clusters will persist. For the same value of the concentration, the size of the cage should be the same, whereas the particles of this glassy system (i.e. the effective clusters) are longer trapped in the cage as the bond lifetime increases (Fig.13).

V I. D I S C U S S I O N A N D C O N C L U S I O N

We have studied a model for gelling systems both in the case of permanent bonds and finite bond lifetime. The study of the dynamics shows that when bonds are permanent (chemical gelation) the divergence of the relaxation time is due to the formation of a macroscopic critical cluster and the decay of the relaxation functions is related to the relaxation of such cluster. In the case of finite b there is an effective cluster size distribution, with a size cutoff. Note that the clusters cannot be easily defined as in the case of chemical gelation: The effective clusters do not coincide with pairwise bonded particles. A cluster can be identified in a statistical sense as a group of monomers which keeps its identity (i.e. the bonds are unbroken) when diffusing a distance of the order of its diameter. The formation of effective clusters leads to an apparent divergence of the relaxation time which is characterized by exponents corresponding to the case of random permanent bonds (random percolation). As the monomer density increases the presence of effective clusters further slows down the dynamics, until a glass transition is reached.

In the case $b \rightarrow 1$, starting with a random configuration of unbonded monomers one obtains an out of equilibrium state as in cluster-cluster aggregation models, which can be representative of colloidal gelation. Ideally this out of equilibrium system is connected to the two lines described above, the pseudo percolation line and the glassy line. The pseudo percolation line can be detected if the effective cluster size is large enough and it is quite distinct from the glassy line. However both lines interfere at low densities and low temperatures with the phase coexistence curve.

We would like to thank K. Dawson, A. de Candia, G. Fof, W. Kob, F. Mallamace, N. Sator, F. Sciortino, P. Tartaglia and E. Zaccarelli for many interesting discussions. This work has been partially supported by a Marie Curie Fellowship of the European Community programme FP5 under contract number HPMF-CI2002-01945, by MIUR-PRIN 2002, MIUR-FIRB 2002, CRdC-AMRA, and by the INFN Parallel Computing Initiative.

[1] P.J.Fly The Physics of Polymer Chemistry Cornell University Press (Ithaca) 1954

[2] P.G.de Gennes Scaling concepts in polymer physics Cor-

- nell University Press (Ithaca) 1980
- [3] M. Adam, D. Lairez, M. Karpasas and M. Gottlieb, *Macromolecules* 30 5920 (1997)
- [4] D. Staufer *Physica A* 106 177 (1981)
- [5] D. Staufer, A. Coniglio and M. Adam, *Adv. in Polymer Sci.* 44 103 (1982)
- [6] J.E. Martin, J.P. Wilcoxon and J. Odinek, *Phys. Rev. A* 43 858 (1991); F. Ikkai and M. Shibayama, *Phys. Rev. Lett.* 82 4946 (1999); S.Z. Ren and C.M. Sorensen, *Phys. Rev. Lett.* 70 1727 (1993); P. Lang. and W. Burdard *Macromolecules* 24 815 (1991)
- [7] A.D. Dinsmore and D.A. Weitz *J. Phys. : Condens. Matter* 14 7581 (2002)
- [8] P. Meakin *Phys. Rev. Lett.* 51 1119 (1983); M. Kolb, R. Botet and R. Jullien *Phys. Rev. Lett.* 51 1123 (1983)
- [9] V. Trappe, V. Prasad, L. Cipelletti, P.N. Segre and D.A. Weitz, *Nature* 411 772 (2001); V. Trappe and D.A. Weitz *Phys. Rev. Lett.* 85 449 (2000)
- [10] H. Gang, A.H. Kral, H.Z. Cummins, and D.A. Weitz, *Phys. Rev. E* 59 715 (1999)
- [11] F. Mallamace, P. Gambadauro, N. Miceli, P. Tartaglia, C. Liao and S.H. Chen, *Phys. Rev. Lett.* 84 (2000) 5431; S.H. Chen, W.R. Chen, F. Mallamace, *Science* 300 (2003) 619
- [12] W. Götze in *Liquid, Freezing and Glass Transition*, eds. J.P. Hansen, D. Levesque and P. Zinn-Justin, Elsevier (1991)
- [13] L. Fabbian, W. Götze, F. Sciortino, P. Tartaglia and F. Thiery, *Phys. Rev. E* 59, R1347 (1999); 60, 2430 (1999); J. Bergenholz, M. Fuchs, and Th. Voigtman, *J. Phys. : Condens. Matter* 12, 6575 (2000)
- [14] K. Dawson, G. Fo, M. Fuchs, W. Götze, F. Sciortino, M. Sperl, P. Tartaglia, Th. Voigtman and E. Zaccarelli, *Phys. Rev. E* 63 011401 (2001); E. Zaccarelli, G. Fo, K.A. Dawson, F. Sciortino and P. Tartaglia, *Phys. Rev. E* 63, 031501 (2001)
- [15] A.M. Puertas, M. Fuchs and M.E. Cates cond-mat/0211087; M.E. Cates to appear in *Annales Henri Poincaré*; A.M. Puertas, M. Fuchs and M.E. Cates *Phys. Rev. Lett.* 88 (2002) 098301
- [16] P.N. Segre, V. Prasad, A.B. Schofeld, and D.A. Weitz *Phys. Rev. Lett.* 86 6042 (2001)
- [17] E. Delgado, A. Fierro, L. de Arcangelis and A. Coniglio *Europhys. Lett.* (2003), in press
- [18] E. Delgado, L. de Arcangelis and A. Coniglio *Eur. Phys. J. B* 2 352 (2000)
- [19] A. Aharony, D. Staufer *Introduction to percolation theory* Taylor and Francis, London (1994)
- [20] I. Carmesin and K. Kremer *Macromolecules* 21 2819 (1988)
- [21] H.P. Deutsch and R. Dickman *J. Chem. Phys.* 93 8983 (1990); H.P. Deutsch and K. Binder *J. Chem. Phys.* 94 2294 (1991)
- [22] E. Delgado, L. de Arcangelis and A. Coniglio *J. Phys. A* 31 1901 (1998); *Europhys. Lett.* 46 288 (1999)
- [23] E. Delgado, L. de Arcangelis and A. Coniglio *Phys. Rev. E* 65 041803 (2002)
- [24] Taking into account both the interaction energy by means of ϵ_b and the frequency f_b for the bonds corresponds to have a free energy barrier in the bond formation [25]: Consider a pair of particles which can be in $+1$ configurations. (unbonded) corresponds to zero energy and 1 (bonded) corresponds to energy $-E_b$. Breaking of a bond corresponds to go from a state of energy $-E_b$ to a state of entropy $S = K \ln \Omega$, with a variation in the free energy $\Delta F = -E_b - K T \ln \Omega$. The lifetime of the bonding configuration is proportional to $e^{\Delta F / K T}$, and the frequency to go from one of the unbonding configurations to the bonding configuration is given by $f_b = \frac{1}{\tau_b}$.
- [25] A. Coniglio, H.E. Stanley, W. Klein *Phys. Rev. B* 25 (1982) 6805
- [26] We consider one starting configuration with a fixed as obtained in the case of permanent bonds. For each value of the bond lifetime τ_b we perform test simulations for different values of f_b . The fraction of formed bonds respect to all the possible ones varies during an initial transient and then fluctuates around an average value which, for a fixed τ_b , depends on ϵ_b and f_b . For the study of the dynamics, for each value of τ_b we take the f_b so that the average value of the fraction of present bonds during the simulations is the same as its value at the same τ_b with permanent bonds.
- [27] The role of directional effects in the attractive interaction in colloidal gels is not clear and is worth to be further investigated.
- [28] R. Jullien and A. Hasegawa *Phys. Rev. Lett.* 74 4003 (1995)
- [29] M. Kolb and R. Jullien, *J. Phys. (Paris) Lett.* 45, L977 (1984); F. Family, P. Meakin, and T. Vicsek, *J. Chem. Phys.* 83, 4144 (1985).
- [30] After having thermalized the system at a given value of the monomer concentration, ϕ , the autocorrelation functions of the density fluctuations, $f_q(t)$, are calculated by time averages over runs of 10^7 MC step/particle. The errors are calculated as the fluctuations on the statistical ensemble ($20-30$ different realizations of the system have been considered). Where not explicitly shown, the error bars are of the order of the symbol size in the figures.
- [31] E. Delgado, A. Fierro, L. de Arcangelis and A. Coniglio in preparation.
- [32] A.T. Ogiński *Phys. Rev. B* 32 7384 (1985).
- [33] A. Parker and V. Normand cond-mat/0306056.
- [34] Although with these two conditions we cannot exclude that we are in an aging regime, we do not expect to find aging, as we are not in the glassy region [31].
- [35] F. Mallamace, S.H. Chen, Y. Liu, L. Lobry and N. Miceli *Physica A* 266 (1999); F. Mallamace, R. Beneduci, P. Gambadauro, D. Lombardo and S.H. Chen, *Physica A* 302 202 (2001)
- [36] F. Laeche, D. Durand and T. Nicolai *Macromolecules* 36 1331 (2003)
- [37] A. Coniglio *J. Phys. : Condensed Matter* 13 9039 (2001)

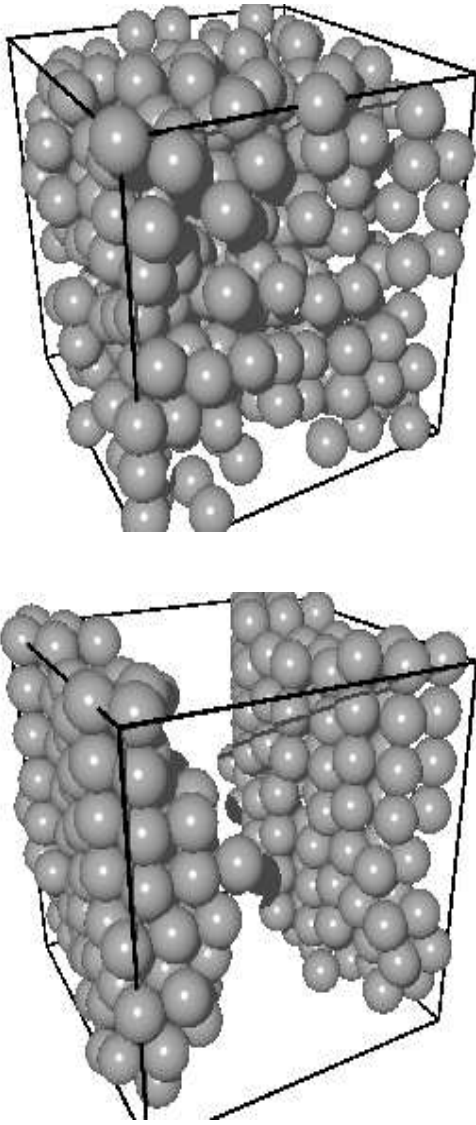


FIG. 1: Two typical configurations obtained for $\phi = 0.6$ with $\phi_b = 100$ and $f_b = 0.02$ (a), where there is no evidence of phase separation, and with $\phi_b = 2$, $f_b = 1$ and monomers of valence 6 (b), where the phase separation occurs.

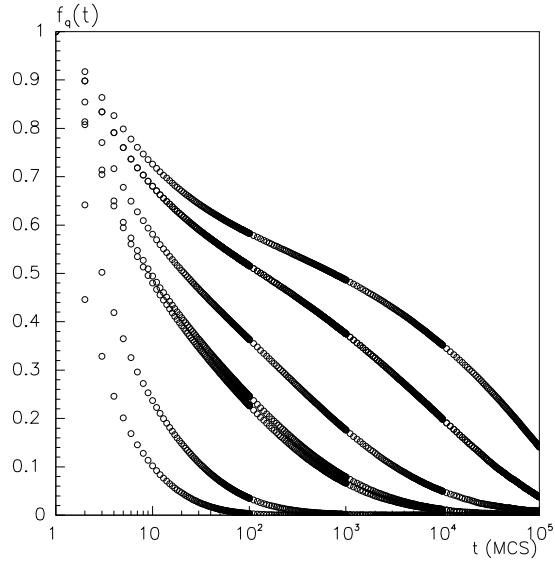


FIG .2: The relaxation functions for permanent bonds $f_q(t)$ as function of the time for $q = 1.36$ and, from left to right, $\phi = 0.5; 0.6; 0.68; 0.718; 0.75; 0.8; 0.85$.

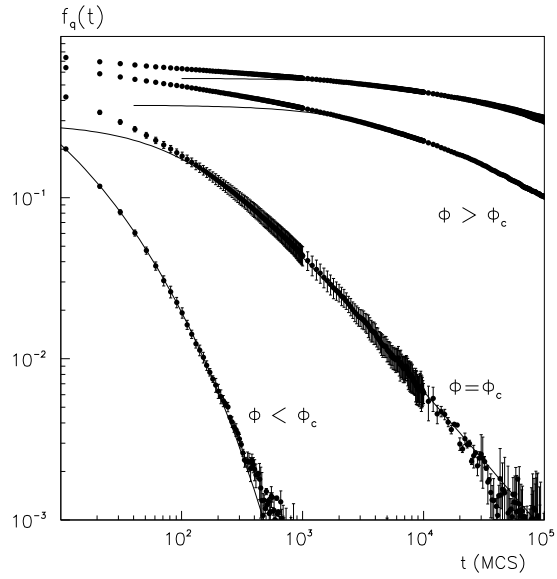
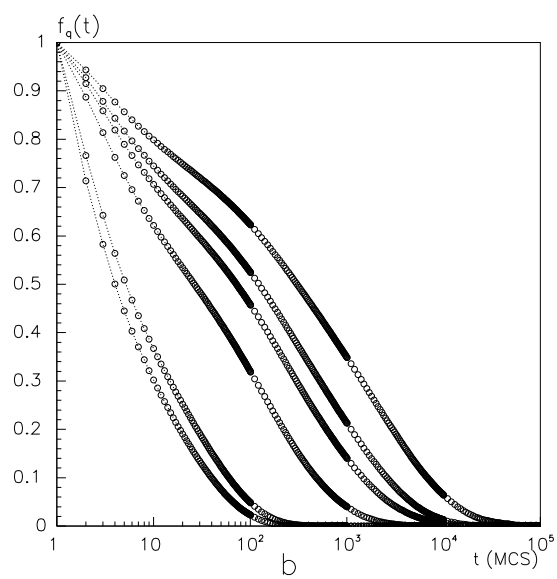
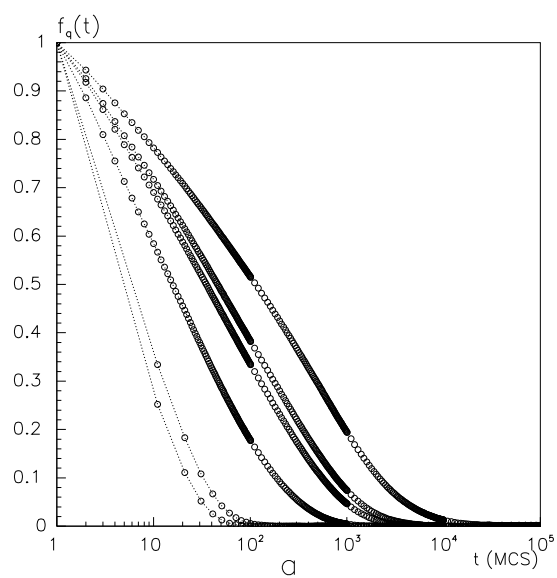


FIG .3: Double logarithmic plot of the autocorrelation functions $f_q(t)$ as function of the time for $q = 1.36$ and $\phi = 0.6; 0.718; 0.8; 0.87$. For $\phi < \phi_c$ the long time decay is well fitted by a function (full line) $e^{-(t/\tau)^{0.3}}$ with $\tau = 0.3$. At the percolation threshold and in the gel phase in the long time decay the data are well fitted by a function $(1 + t/t_0)^{-c}$.



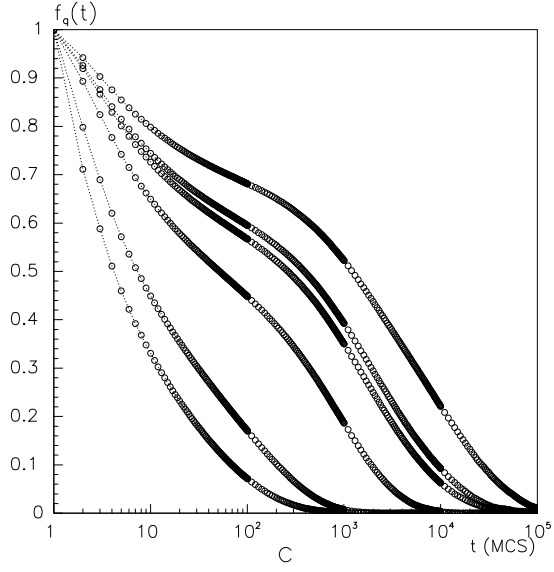


FIG. 4: $f_q(t)$ as function of the time for $q = 1.36$ calculated on a cubic lattice of size $L = 16$: for $b = 0.6; 0.7; 0.8; 0.85; 0.87; 0.9$ (from left to right) and $b = 10M$ C step=particle (a); $b = 100M$ C step=particle (b); $b = 1000M$ C step=particle (c); the dotted lines are a guide to the eye.

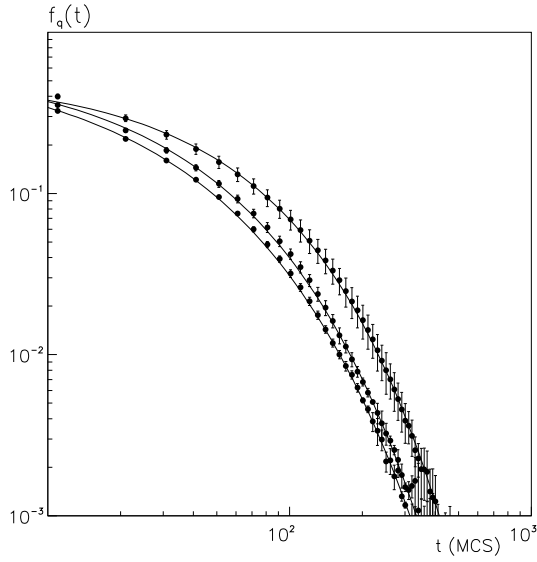


FIG. 5: The long time decay of $f_q(t)$ in a log-log plot for $q = 1.36$. It has been calculated on a cubic lattice of size $L = 16$ for $b = 100M$ C step=particle (from left to right $b = 0.65; 0.68; 0.718$). The data are fitted using a stretched exponential function with $\alpha = 0.7$ (full lines).

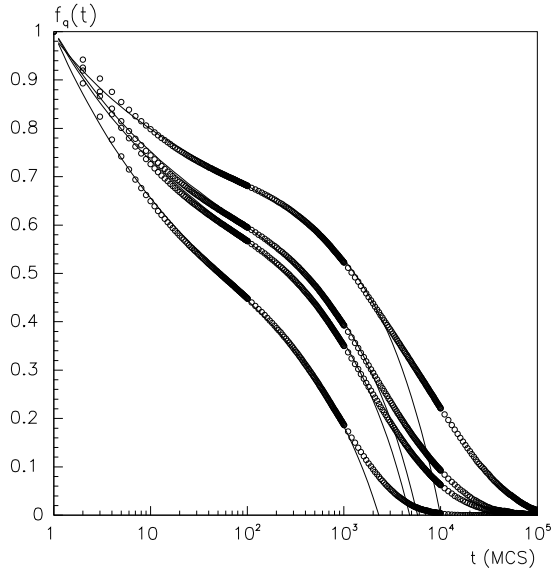


FIG. 6: $f_q(t)$ as function of the time for $q = 1.36$ calculated on a cubic lattice of size $L = 16$ for $b = 1000$ C step=particle. From left to right $q = 0.8; 0.85; 0.87; 0.9$. The full lines correspond to the t with the $-$ correlator.

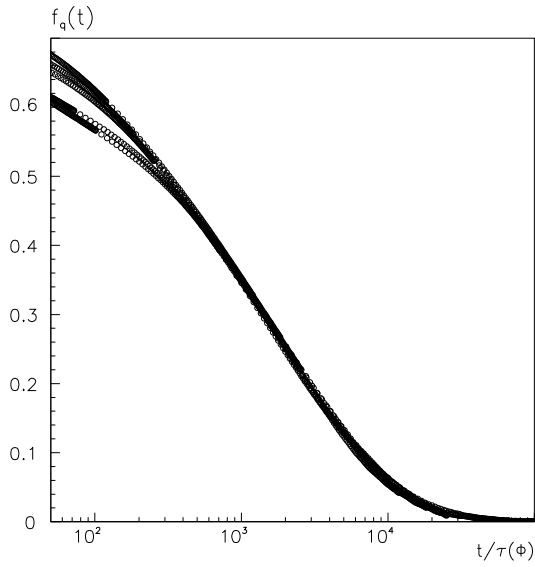


FIG. 7: $f_q(t)$ obtained for $q = 1.36$, $b = 1000$, and $q = 0.85; 0.87; 0.9; 0.91; 0.92$: by opportunistically rescaling them by a quantity $\tau(\Phi)$ they collapse into a unique master curve, well fitted by a stretched exponential function with $\alpha = 0.5 \pm 0.06$.

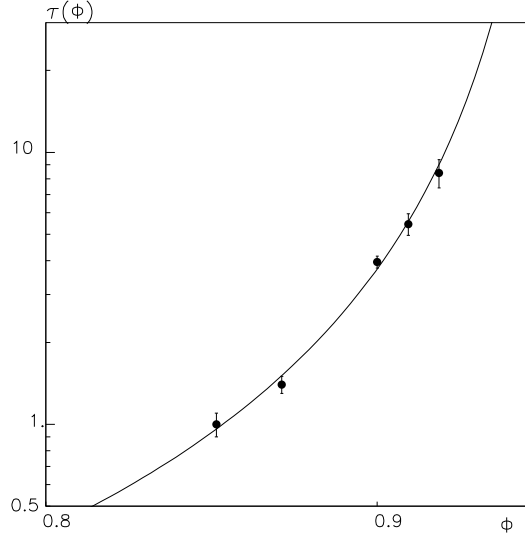


FIG. 8: Log-log plot of the characteristic time $\tau(\phi)$ obtained by the rescaling of the relaxation functions. The points have been fitted (full line) with the function $0.006(\phi - \phi_c)^{2.33}$, where $\phi_c = 0.96 \pm 0.01$.

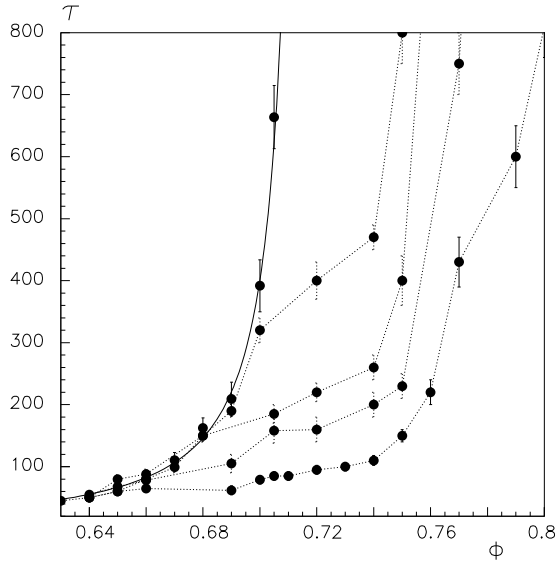


FIG. 9: The average relaxation time as function of the density; from left to right: the data for the permanent bond case diverge at the percolation threshold with a power law (the full line); the other data refer to finite $N_b = 3000; 1000; 400; 100$ (the dotted lines are a guide to the eye). The apparent divergence of the relaxation time, τ , is observed at the percolation threshold of the permanent bond case, $\phi_c = 0.718$, for all the values of N_b .

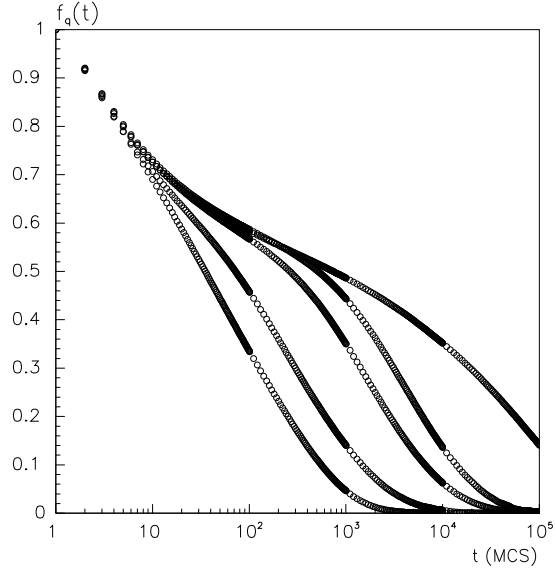


FIG. 10: $f_q(t)$ obtained for $\beta = 0.85$ and $q = 1.36$: the different curves refer to $b = 10; 100; 400; 1000$, compared to the permanent bond case (from left to right).

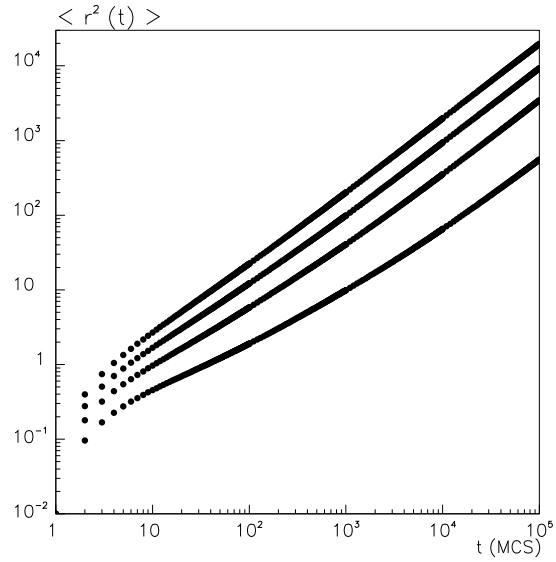


FIG. 11: The mean-square displacement $\langle r^2(t) \rangle$ of the particles as function of the time in a double logarithmic plot for permanent bonds: from top to bottom $\beta = 0.4; 0.5; 0.6; 0.7$, approaching β_c .

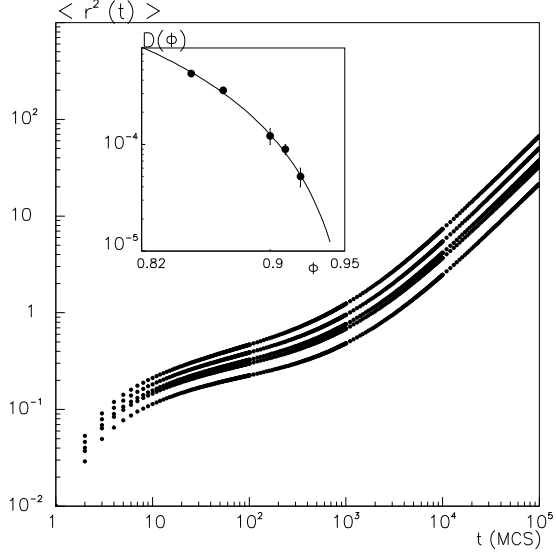


FIG. 12: The mean-square displacement $\langle r^2(t) \rangle$ of the particles as function of the time in a double logarithmic plot for $\phi_b = 1000$ MCS per particle: from top to bottom $\phi = 0.8; 0.82; 0.85; 0.87; 0.9$, approaching $\phi_g(\phi)$. In the inset, the diffusion coefficient: the full line is the fit with the function $(0.963 - \phi)^{2.13}$.

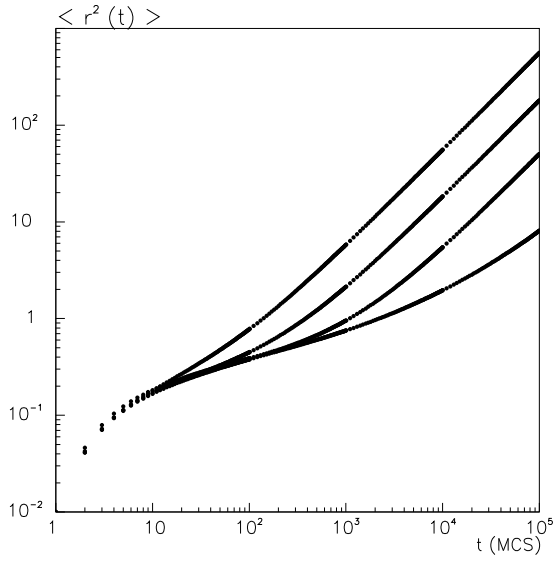


FIG. 13: The mean-square displacement $\langle r^2(t) \rangle$ of the particles as function of the time in a double logarithmic plot, obtained at $\phi = 0.85$. The different curves, from top to bottom, refer to $\phi_b = 10; 100; 1000$ and the case of permanent bonds.